

Raman Spectroscopic Study on Hydrogen Bonding in Recovered Ice IV

Christoph G. Salzmann, Ingrid Kohl, Thomas Loerting, Erwin Mayer, and Andreas Hallbrucker*

Institut für Allgemeine, Anorganische und Theoretische Chemie, Universität Innsbruck, A-6020 Innsbruck, Austria

Received: June 28, 2002; In Final Form: October 31, 2002

Ice IV was prepared in a reproducible manner on heating high-density amorphous ice (HDA) at pressure of 0.81 GPa up to ≈ 162 K at a slow rate of ≈ 0.5 K min^{-1} , quenching thereafter to 77 K, and recovering the sample under liquid N_2 at 1 bar. Recovered ice IV was characterized by X-ray diffraction and it was free of HDA or of low-density amorphous ice. D_2O ice IV contained no crystalline impurities, whereas the H_2O sample contained a minor impurity of ice XII. D_2O ice IV with 11 mol % HOD and H_2O ice IV with 9.0 mol % HOD were studied in vacuo by Raman spectroscopy between 80 and 145 K. The decoupled O–D (O–H) stretching band in H_2O (D_2O) ice IV consists of two overlapping peaks centered at 2500 (3390) and 2458 (3322) cm^{-1} at 80 K. Peak maximum of the coupled O–H (O–D) stretching band region is at 3200 (2360) cm^{-1} . At low frequency a band at ≈ 498 (≈ 365) cm^{-1} is assigned to a librational mode, whereas bands at ≈ 252 (≈ 250), 208 (203), 178 (172), 152 (149) and 126 (123) cm^{-1} originate from translation modes. On heating ice IV, we measured the development of peak-positions and the phase transition from ice IV to ice I. We did not observe indication for formation of an amorphous phase during this transition. Curve resolution of the decoupled O–D stretching transition region into two component bands is consistent with the assignment of the high-frequency band centered at 2500 cm^{-1} to the O–D \cdots O H-bonds with 2.88 and 2.92 Å length, and of the low-frequency component band centered at 2458 cm^{-1} to H-bonds with 2.79 and 2.81 Å length. The composite band shape is consistent with large fwhh's (full width at half-heights) of the distinct bands from the four types of H-bonds.

1. Introduction

Ice IV is a metastable high-pressure phase of ice.^{1–9} Its existence was first suspected in 1912 and later verified by Bridgman.^{1,2} It can be formed from liquid water in the pressure range from 0.2 to 1.0 GPa (shown in Figure 1 of ref 8) which covers most of the pressure range of the stability domains of stable ices III, V, and VI. Although the nucleation of ice IV can be induced by appropriate nucleating agents,^{3,4} its formation seems to have been a random event.^{4,8} Recently we showed that pure ice IV can be formed in a reproducible manner on controlled isobaric heating of high-density amorphous ice (HDA) at 0.81 GPa up to ≈ 195 K.¹⁰ This approach is complementary to formation of ice IV on cooling liquid water under pressure, and it offers the possibility to obtain pure ice IV in gram quantities. The key parameter in our preparation is the heating rate, with slow heating rates favoring formation of ice IV, whereas fast heating rates lead to the formation of also metastable ice XII. Ice IV can be recovered by quenching to 77 K and release of pressure.^{4,10} Recovered ice IV is fully proton-disordered according to diffraction,⁵ infrared,¹¹ and thermodynamical considerations.⁴

The structure of ice IV is based on a rhombohedral unit cell which contains 16 water molecules with 12 oxygen atoms O(1) in a general position, and 4 oxygen atoms O(2) in a special position.⁵ These oxygens are tetrahedrally connected with their neighbors through asymmetric hydrogen bonds producing four nonequivalent H-bonded O–O distances: The first type of

O(1)–O(1') H-bonds assemble a puckered six-ring. A second H-bond of type O(2)–O(2') passes through the center of each ring. These two H-bonds are lengthened considerably to 2.88 and 2.92 Å relative to the H-bonds in ice I (2.75 Å) through repulsion between O(1) and O(2) at nonbonded distances. The remaining two H-bond distances of 2.79 Å for type O(1)–O(2'') and of 2.81 Å for of O(1)–O(1''') are far more shorter. Bond bending in ice IV is relatively low compared to other high-pressure ice phases.^{5,12}

Here we report the Raman spectra of H_2O ice IV containing 5.0 wt % D_2O , and of D_2O ice IV containing 5.0 wt % H_2O , which were recorded in vacuo at temperatures between 80 and 145 K. The decoupled O–D (O–H) stretching transitions of HOD molecules in a lattice of a H_2O (D_2O) ice IV crystal can be used as a probe for hydrogen bonding with neighboring molecules and for hydrogen-bonded O–H \cdots O (O–D \cdots O) distances.^{13–16} The changes in peak positions through heating of the ice IV sample were recorded, as well as the phase transition of ice IV to ice I. We did not observe any indication of formation of an amorphous phase as intermediate during the ice IV \rightarrow ice I phase transition. With this report we complete the set of Raman spectra of all currently known ice polymorphs from ices I_h and I_c to ice XII.^{17–27}

2. Experimental Section

The procedure of preparing ice IV on isobaric heating of HDA is described in detail in ref 10. Briefly, 0.300 cm^3 of either D_2O water (from Aldrich, no. 15,188-2, 99.9 atom % D) containing 5.0 wt % H_2O , or of deionized H_2O water with 5.0 wt % D_2O , was pipetted into an indium cup in a precooled piston–cylinder

* To whom correspondence should be addressed. E-mail: andreas.hallbrucker@uibk.ac.at.

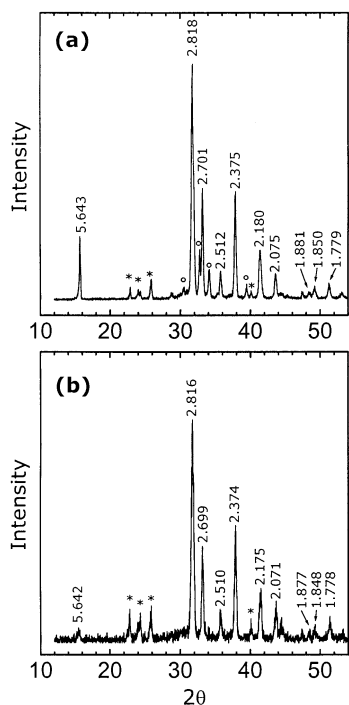


Figure 1. (a) X-ray diffractogram (Cu-K α) of an H_2O ice IV sample containing a small amount of ice XII (marked by open circles) with d spacings in Å , and (b) of a pure D_2O ice IV sample. The samples were recovered after decompression under liquid N_2 and diffractograms recorded at 80 K. Bragg peaks of ice Ih from condensation of water vapor during the transfer of the sample are marked with asterisks.

apparatus with an 8-mm diameter piston. HDA was then made by compression of ice Ih at 77 K up to 1.6 GPa using a computerized “universal testing machine” (Zwick, model BZ100/TL3S) at a rate of 7000 N min^{-1} . Its positional reproducibility is $\pm 5 \text{ }\mu\text{m}$, and the spatial resolution of the drive is $0.01 \text{ }\mu\text{m}$. Pressure–displacement curves indicating the phase transition to HDA were recorded with the TestXpert 7.1 software of Zwick and were identical to those reported elsewhere.^{10,28–30} HDA was then transformed to ice IV on isobaric heating at a rate of $\approx 0.5 \text{ K min}^{-1}$ from 77 K to $\approx 162 \text{ K}$ at a pressure of 0.81 GPa.¹⁰ The progress of the phase transition was monitored by displacement–temperature curves. After complete crystallization, the sample was quenched to 77 K under pressure and then recovered under liquid N_2 after release of pressure. Recovered ice IV was characterized by X-ray diffraction as shown in Figure 1a,b. Raman spectra were recorded on a Labram-1B spectrometer equipped with a microscope (from Dilor company), through an ULWD-50 objective (Olympus company), by coadding four sets of spectra with overall recording time of $\approx 10 \text{ min}$. A 20 mW He–Ne Laser with 632.8 nm wavelength was used, and the 1800 L/mm grating provides a resolution of 1.1 cm^{-1} at 150 cm^{-1} increasing to 0.6 cm^{-1} at 3600 cm^{-1} . The abscissa was calibrated with a silicon standard, and the sharp Raman shifts are accurate to $\pm 2 \text{ cm}^{-1}$. Relative intensities of bands in different parts of the Figures are not shown on the same scale. An Oxford Microstat was used as cryostat. Temperature of the sample was controlled by a LakeShore CI330 autotuning temperature controller and remained constant within $\pm 0.2 \text{ K}$. Spectra were recorded in vacuo at $\approx 10 \text{ mbar}$.

X-ray diffractograms were recorded on a diffractometer in θ – θ geometry (Siemens, model D 5000, Cu K α), equipped with a low-temperature camera from Paar. The sample plate was in horizontal position during the whole measurement. Installation of a “Goebel mirror” allowed to record small amounts of sample without distortion of the Bragg peaks.

3. Results and Discussion

A major effort was to prepare ice IV samples with a minimal degree of impurities, such as HDA or ice XII. This turned out to be essential because upon recording of a Raman spectrum through a microscope, the laser beam is highly focused and high spatial resolution in the μm range is obtained. Thus, the Raman spectrum depends on where the sample is excited, and it is easily possible to obtain exclusively spectra of an impurity.²⁰ To estimate the degree of impurities in a sample, X-ray diffractograms of the ice IV samples were recorded as shown in Figure 1.

The diffractogram of D_2O ice IV (b) contains no impurities, whereas the H_2O sample (a) shows a minor ice XII impurity whose Bragg reflections are marked by open circles. The d spacings of ice XII are about the same as those reported by Lobban et al.¹² and by Koza et al.³¹ As we will show later, the Raman spectra of H_2O ice IV can be easily distinguished from those spectra of the ice XII impurities. Raman spectra of ice XII are shown in Figure 2 of ref 20. Bragg peaks marked with asterisks are from a small amount of ice Ih which had condensed onto the sample during transfer.

Figure 2 shows three spectral regions of the Raman spectra of H_2O ice IV containing 9.0 mol % HOD (top), and of D_2O ice IV containing 11 mol % HOD (bottom). These concentrations were obtained by adding 5.0 wt % of D_2O (H_2O) to H_2O (D_2O).^{13,14} The spectra were recorded at 80 K and $\approx 10 \text{ mbar}$. Spectra a and d (left) show the coupled O–H (O–D) stretching transition region with the peak maximum at 3200 (2360) cm^{-1} and shoulders at ≈ 3330 and ≈ 3420 (≈ 2495) cm^{-1} . Spectra b and e (middle) show the decoupled O–D (O–H) stretching transitions with two overlapping peaks centered at 2458 and 2500 (3322 and 3390) cm^{-1} . The low-frequency region (c) and (f) (right) contains peaks centered at ≈ 498 , ≈ 252 , 208 , 178 , 152 , and 126 cm^{-1} for H_2O ice IV, and at ≈ 365 , ≈ 250 , 203 , 172 , 149 , and 123 cm^{-1} for D_2O ice IV. Two sharp lines marked by asterisks at 180.4 and 136.1 cm^{-1} are plasma lines from the He–Ne laser. The two peaks at higher frequencies are relatively broad compared to the four sharp peaks at lower frequencies for both, H_2O and D_2O ice IV. This characteristic low-frequency spectrum which could be denoted as a “fingerprint region”, allows effective distinction from other ice modifications,¹⁸ e.g., from ice XII which shows only one broad translational mode centered at 195 cm^{-1} .²⁰

The ratios of the peak frequencies of the coupled O–H/O–D stretching bands and of the two peak positions of the decoupled O–H/O–D stretching bands are close to the square root of 2 (1.356 for coupled, 1.356 and 1.352 for decoupled frequencies). This is as expected for motions determined primarily by the hydrogen or deuterium nuclei.^{13–15} Likewise, the $\text{H}_2\text{O}/\text{D}_2\text{O}$ peak frequency ratio of the broad band at $\approx 498 \text{ cm}^{-1}$ for H_2O and at $\approx 365 \text{ cm}^{-1}$ for D_2O is 1.36 which is close to $\sqrt{2}$ ($=1.41$). This allows its assignment to a librational mode. The $\text{H}_2\text{O}/\text{D}_2\text{O}$ peak frequency ratios of the peaks centered at 252 , 208 , 178 , 152 , and 126 cm^{-1} to those at 250 , 203 , 172 , 149 and 123 cm^{-1} are: 1.01, 1.02, 1.03, 1.02, and 1.02. All these values are close to the square root of the ratio of molecular masses, $\sqrt{(20/18)}$ ($=1.05$). This shows that these modes involve the motion of whole water molecules and therefore must be assigned to translational modes.¹⁵

Compared to other ice polymorphs,¹⁸ the multitude of peaks in the low-frequency region of ice IV is remarkable. In ref 18 Minceva-Sukarova et al. state that the variety of O–O distances and O–O–O angles in the different ices enriches the lattice vibration spectrum. So the noticeable structural variety in ice

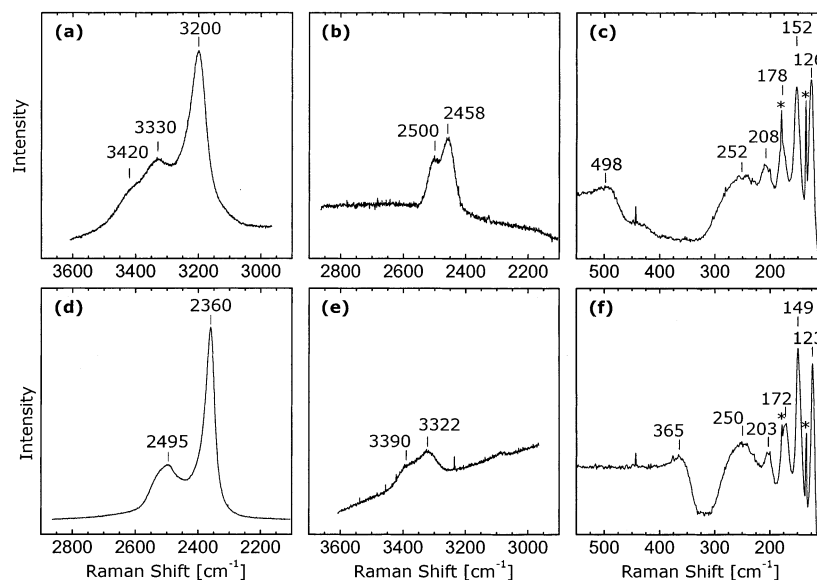


Figure 2. Raman spectra of ice IV recorded at 80 K. (a) On top three spectral regions of H₂O ice XII containing 9.0 mol % HOD are shown, and below the corresponding spectral regions of D₂O ice XII containing 11 mol % HOD. Left: the coupled O–H (O–D) stretching transition region with the peak maximum at 3200 (2360) cm⁻¹. Middle: the decoupled O–D (O–H) stretching transition with peak maxima at 2458 and 2500 (≈3322 and ≈3390) cm⁻¹. Right: the low-frequency region with peaks at ≈498, ≈252, 208, 178, 152, and 126 cm⁻¹ for H₂O ice IV, and at ≈365, ≈250, 203, 172, 149 and 123 cm⁻¹ for D₂O ice IV. Two sharp lines at 180.4 and 136.1 cm⁻¹ (marked by asterisks) are plasma lines. The ordinate scale differs for each spectral region.

IV⁵ might be the origin of the observed multitude of peaks. However, to our knowledge, a lattice dynamical calculation on ice IV has not been published so far. A detailed assignment of translational vibrations for ordered ice VIII is given by Wong and Whalley,¹⁹ and for disordered ice I_h and I_c by Whalley and Bertie.³²

Two (one) more samples of H₂O (D₂O) ice IV were studied and spectra were recorded for each sample at several different locations of the laser spot. These additional spectra were identical within experimental error with respect to peak positions and relative intensities with those depicted in Figure 2. Thus, Figure 2 represents the Raman spectra of polycrystalline ice IV. However, in some cases the relative intensities of the low-frequency bands varied strongly and thus, differed from those depicted in Figure 2. This was often accompanied by a change in the intensities of the decoupled O–D stretching transitions and a slight increase of the feature at 3330 cm⁻¹ (not shown). Presumably in these cases the laser beam was directed at a large crystal face, and polycrystallinity of the sample was not guaranteed for the whole micrometer-sized laserspot. But in most cases these regions could be avoided by checking the shape and reflection properties of the laserspot on a TV monitor. The same phenomenon has been described by Bertie and Francis for Raman spectra of ice II.²⁷

In a recent study of HDA by Yoshimura and Kanno³³ Raman spectra taken at ≈1.2 GPa and temperatures of 218, 267 and 288 K were assigned to ice IV. As in this p–T region ice VI is the stable phase, which was pointed out also in Figure 1 of ref 33, it was ascertained with the corresponding author³⁴ that ice VI was erroneously marked as ice IV on page 54 of their paper.

Figure 3 shows the development of the coupled O–H stretching transitions (left), the decoupled O–D stretching transitions (middle) and the low-frequency modes (right) of H₂O ice IV on heating from 80 K up to 145 K. Spectra were recorded at temperatures as indicated at the left of each spectrum starting from 80 K. Heating rate to subsequent temperatures was about 2 K min⁻¹. After reaching a certain temperature, recording of a spectrum was started after two minutes in order to ensure

thermal equilibration of the sample. During the phase transition at ≈140 K, reflection conditions for the laser beam changed so much that only the most intense feature, the coupled O–H stretching transition, could still be observed.

The sharp peak maximum of the coupled O–H stretching band (left) shifts on heating from 3200 cm⁻¹ at 80 K (marked by the dotted line) to 3209 cm⁻¹ at 135 K. On further heating to 140 K, a second peak develops on the low-frequency side which is attributed to ice I. This is clearly seen by the second dotted line at 3108 cm⁻¹. The difference between ice I_h and ice I_c cannot be established by means of Raman spectroscopy,^{14,35} but most presumably ice IV (like most other high-pressure ice polymorphs^{36,37}) transforms first to cubic ice (ice I_c) at atmospheric pressure. Phase transition of ice IV to ice I_c is complete at 145 K. We emphasize that the spectrum at 140 K shows the simultaneous existence of ice IV and ice I_c. This indicates further that ice IV transforms directly into ice I_c and not via some amorphous phase.

The strong Raman band centered at 3200 cm⁻¹ in the spectrum of coupled O–H stretching transition (at 2360 cm⁻¹ for coupled O–D) is probably due to ν₁ vibrations of water molecules which are vibrating largely in phase with one another.³⁵ Similar assignment has been proposed for other high-pressure ices such as ice VIII,¹⁹ ice II and ice IX,²⁷ and ice XII.²⁰

The peak positions of the decoupled O–D stretching bands (middle) increase during heating from 2458 and 2500 cm⁻¹ at 80 K to 2462 and 2507 cm⁻¹ at 135 K. The full width at half-height (fwhh) of the composite band profile increases slightly from 82 cm⁻¹ at 80 K to 85 cm⁻¹ at 135 K. The peak frequency of the decoupled O–D stretching transition of ice I_c at 145 K is centered at 2424 cm⁻¹ and agrees with that reported in the literature.^{14,38}

Referring to Figure 6 and Tables 1 and 2 in ref 18, the coupled O–H or decoupled O–D stretching bands of various ice polymorphs show a decrease of frequency when the applied pressure is increased. This behavior can qualitatively be explained by the increasing attraction of O_B for H_A in a O_A–

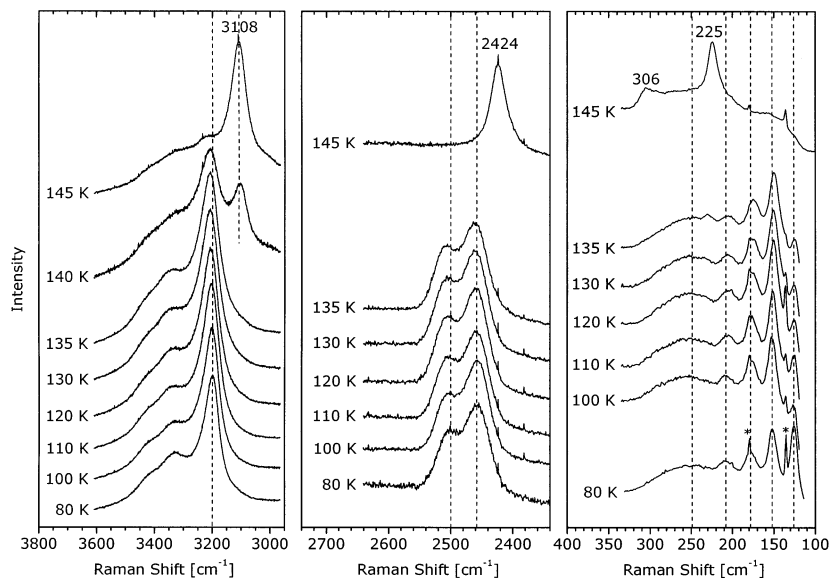


Figure 3. The temperature dependence of the peak frequencies of H₂O ice IV containing 9.0 mol % HOD, and the transition to ice I. The spectra are shifted vertically for clarity.

H_A⋯O_B hydrogen bond which results in a stronger hydrogen bond, but weaker O_A–H_A bond. Consequently, a weaker O_A–H_A bond results in a lower stretching frequency.¹⁵ In our experiment the hydrogen bonds lengthen due to the thermal expansion of the solid. Considering the above explanation, the observed positive $(d\nu/dT)_p$ value for the O–H (O–D) stretching bands of ice IV is expected and it is consistent with positive $(d\nu/dT)_p$ observed for the other high-pressure forms of ice. (cf. Tables 1 and 2 in ref 18)

In contrast to the coupled O–H and decoupled O–D stretching bands, the sharp translational modes (right) show a negative $(d\nu/dT)_p$ value. Their frequencies decrease from 208, 178, 152, and 126 cm^{−1} at 80 K to 205, 175, 150, and 125 cm^{−1} at 135 K. The intensity of the lowest frequency peak diminishes during heating because of the intensity cutoff of the notch filter which limits the measurements at low frequencies. At 145 K the typical spectra of ice I_c with peak frequencies at 225 and 306 cm^{−1} were measured. Because this spectral region was measured last at each indicated temperature, the 225 cm^{−1} peak of ice I_c can already be seen weakly in the spectrum recorded at 135 K. Negative $(d\nu/dT)_p$ values for the translation bands as measured in ice IV, have also been reported for the translation bands of other ice polymorphs (cf. Table 1 in ref 22).

X-ray studies showed that D₂O Ice IV contains four different types of O–D⋯O hydrogen bonds, with distances of 2.916, 2.880, 2.805, and 2.785 Å and multiplicities of 1, 6, 3, and 6 (Table 5 in ref 5). It is believed that all hydrogen atoms in ice IV are positionally disordered.^{4,5,11} The decoupled O–D (O–H) stretching transition of HDO in a dilute solution in H₂O (D₂O) ice IV crystals may be used as a probe to test for various molecular environments in an H₂O (D₂O) crystal.^{13–15} The peak frequencies of decoupled O–D (O–H) stretching vibrations are largely determined by variations in the static perturbations they experience, and in ice, hydrogen bonds to neighboring molecules account for most of this perturbation.^{15,39} The dominant parameter which is correlated with the peak frequency of a decoupled O–D (O–H) stretching band is the O–H⋯O (O–D⋯O) bond length, and several correlations have been reported (reviewed in ref 39). In general a longer O–H⋯O distance corresponds to a higher peak frequency, whereas shorter O–H⋯O distances produce lower frequencies. A correlation based

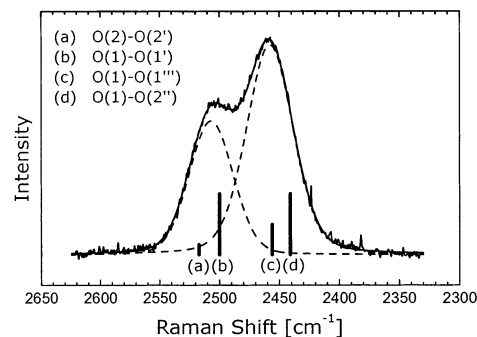


Figure 4. The Raman spectrum of the bands due to the decoupled O–D stretching transition in H₂O ice IV containing 9.0 mol % HOD (recorded at 110 K). The spectrum is baseline-corrected by a two-point baseline with breakpoints at 2630 and 2320 cm^{−1}. Bar graphs show the peak frequencies as calculated from eq 1. Relative heights of the bars indicate the different multiplicities of the four types of H-bonds. The inset assigns the bars to the different bond types. The two peaks with dashed lines are the results of peak fitting with two mixed Gauss–Lorentz profile functions. Peak maxima are at 2507 and 2458 cm^{−1} and fwhh are 43 and 46 cm^{−1}. The sum of both fitted peaks is shown by a solid line.

on extensive ice VII data was proposed by Tulk et al.¹⁶ and will be used in the following (eq 1),

$$\nu_{\text{OD}} = 2782.1 - 1560.1 \exp(-R/1.474) - 269251.6 \exp(-R/0.9938)^2 \quad (1)$$

where ν_{OD} is the frequency of the decoupled O–D peak and R the mean O–H⋯O distance.

The bandwidth also contains information about environments of the HDO molecules. For example, the fwhh of a decoupled O–D stretching transition in proton-ordered H₂O ice II is only ≈ 5 cm^{−1}, but it is ≈ 30 cm^{−1} in disordered ice I.^{14,15} This had been attributed by Bertie and Whalley¹⁴ to disorder in the positions of the oxygen atoms in ice I and confirmed subsequently in neutron diffraction studies by Kuhs and Lehmann (reviewed in ref 39).

Figure 4 displays the bands due to the decoupled O–D stretching transition region in ice IV where the sloping background had been subtracted. To be consistent with the X-ray study of ice IV,⁵ we present the spectrum recorded at 110 K.

By inserting the four different O—O distances of ice IV for the four types of hydrogen bonds into eq 1, we obtain four peak frequencies: 2517, 2500, 2456, and 2441 cm^{-1} . These frequencies are shown as a bar graph in Figure 4. The relative heights of the bars indicate the multiplicity of the different H-bond types which are listed in the insert. These calculated frequencies and their intensities agree very well with the position and the shape of the composite band profile of the spectrum. No other features than the two overlapping peaks are detectable. So it is plausible that the band at 2500 cm^{-1} is a superposition of peaks a and b, whereas the band at 2458 cm^{-1} corresponds to peaks c and d.

Fairly artifact-free subtraction of a baseline is necessary before curve resolution becomes meaningful. We used a two-point baseline to subtract the sloping background, with break points set at 2630 and 2320 cm^{-1} . These break-point positions are sufficiently separate from the peak maxima to ensure that wings of Lorentzian band profiles are not cut off. The effect of baseline correction was further controlled by comparing the second-derivative curve of the spectrum with that of the background-corrected composite band profile, and by aiming for their optimal superposition as outlined in ref 40. A curve fit with two mixed Gauss–Lorentz sum profile functions was performed and the two resulting curve-fitted peaks are shown with dashed lines in Figure 4. The sum of both fitted peaks is represented by a solid line which fits very well to the measured spectrum. The fitted peaks are centered at 2507 (11% Lorentz) and 2458 cm^{-1} (23% Lorentz) and have a fwhh of 43 and 46 cm^{-1} . For spectra of low signal-to-noise ratio such as that shown in Figure 4, reliable resolution of overlapping bands into the component bands requires that separation of peak maxima is larger than the mean fwhh.^{40–42} This requirement is fulfilled in our curve fit because separation of peak maxima is 49 cm^{-1} and the average fwhh is $\approx 44 \text{ cm}^{-1}$. The relative intensities of the two fitted peaks centered at 2507 and 2458 cm^{-1} is 0.57 to 1. Further curve fits of the decoupled O–D stretching of all Raman spectra of ice IV shown in Figure 3 give an average relative intensity of 0.52 ± 0.09 . A systematic temperature dependence could not be observed.

In a next step we estimate what the minimal fwhh of the four calculated bands at frequencies a and b, and at c and d, has to be in order to obtain the type of overlap seen in the Raman spectrum. Separation between peak frequencies a and b is 17 cm^{-1} and between c and d it is 15 cm^{-1} . Whether or not the two peaks centered at c and d overlap completely or can be identified by two distinct peaks or by a shoulder on a peak, depends on their peak separation, their fwhh's, their relative intensities, and the band shape. In Figure 7 of ref 40 synthetic curves of two overlapping bands of Gaussian band shape are shown, where the degree of overlap is varied. In the middle section of this figure, the relative intensity of the two bands is 2:1, which is the same ratio as peaks d to c in our Figure 4. In this Figure 7, the low-intensity band can be identified as a distinct shoulder when the separation of their peak maxima is equal to their mean fwhh's, whereas the shoulder disappears completely when separation of peak maxima is 0.83 times their mean fwhh's. This implies for c and d centered at 2456 and 2441 cm^{-1} in our Figure 4, that two distinct bands can be identified when their mean fwhh's is $\leq 15 \text{ cm}^{-1}$, but that only one band becomes observable when it is $\geq 18 \text{ cm}^{-1}$. The latter situation applies for c and d comprising the curve-fitted band centered at 2458 cm^{-1} , and in the same manner for a and b comprising the curve-fitted band centered at 2507 cm^{-1} . Thus, the minimal fwhh's of the calculated bands (c) and (d) has to be clearly much larger than that of $\approx 5 \text{ cm}^{-1}$ observed for proton-

ordered H₂O ice II,^{14,15} and accordingly, ice IV is proton-disordered. However, we would probably not be able to detect a minor amount of proton-ordering in disordered ice IV in this way. We note that the distinct features of the calculated bands a–d might become observable in fourth-derivative curves once IR spectra of very high signal-to-noise ratio are available, in the manner shown in ref 40 for highly overlapping bands.

The sum of multiplicities of frequencies a and b is 7, and for frequencies c and d it is 9, while the ratio of the areas of the two curve-fitted peaks gives a value of 5.1 to 9. The two overlapping component bands are close enough that experimental parameters affecting their relative intensity such as laser frequency or detector sensitivity can be expected to be identical. Therefore, if our assignment is correct, we would expect relative intensities of the bands to be 7 to 9, instead of the 5.1 to 9 ratio observed here. This can be understood by assuming that the relative scattering cross sections differ; that is, that the band at higher frequency has a lower relative scattering cross section than that at lower frequency.⁴³

Concerning the proton ordering in ice IV, we emphasize the lack of sharp bands or of shoulders in the decoupled O–D stretching transition attributable to the four distinct O–D···O hydrogen bonds. Sharp bands in the decoupled O–D, O–H stretching transition region would indicate an ordered structure as in ice II or IX.¹⁸ Hence, consistent with previous studies^{4,5,11} we conclude ice IV to be proton-disordered. However, final proof of this conjecture could only be obtained by neutron diffraction studies.

Acknowledgment. Financial support of the “Forschungsförderungsfonds” of Austria, project P13930-PHY is acknowledged.

References and Notes

- (1) Bridgman, P. W. *Proc. Am. Acad. Arts Sci.* **1912**, *47*, 441.
- (2) Bridgman, P. W. *J. Chem. Phys.* **1935**, *3*, 597.
- (3) Evans, L. F. *J. Appl. Phys.* **1967**, *38*, 4930.
- (4) Engelhardt, H.; Whalley, E. *J. Chem. Phys.* **1972**, *56*, 2678.
- (5) Engelhardt, H.; Kamb, B. *J. Chem. Phys.* **1981**, *75*, 5887.
- (6) Mishima, O.; Stanley, H. E. *Nature* **1998**, *392*, 164.
- (7) Chou, I.-M.; Blank, J. G.; Goncharov, A. F.; Mao, H.-K.; Hemley, R. J. *Science* **1998**, *281*, 809.
- (8) Chou, I.-M.; Haselton, H. T. *Rev. High-Pressure Sci. Technol.* **1998**, *7*, 1132.
- (9) Petrenko, V. F.; Whitworth, R. W. *Physics of Ice*; Oxford University Press: Oxford, 1999.
- (10) Salzmann, C. G.; Loerting, T.; Kohl, I.; Mayer, E.; Hallbrucker, A. *J. Phys. Chem. B* **2002**, *106*, 5587.
- (11) Engelhardt, H.; Whalley, E. *J. Chem. Phys.* **1979**, *71*, 4050.
- (12) Lobb, C.; Finney, J. L.; Kuhs, W. F. *Nature* **1998**, *391*, 268.
- (13) Haas, C.; Hornig, D. F. *J. Chem. Phys.* **1960**, *32*, 1763.
- (14) Bertie, J. E.; Whalley, E. *J. Chem. Phys.* **1964**, *40*, 1637.
- (15) Eisenberg, D.; Kauzmann, W. *The Structure and Properties of Water*; Plenum Press: New York, 1969; Vol. 1.
- (16) Tulk, C. A.; Klug, D. D.; Branderhorst, R.; Sharpe, P.; Ripmeester, J. A. *J. Chem. Phys.* **1998**, *109*, 8478.
- (17) Taylor, M. J.; Whalley, E. *J. Chem. Phys.* **1963**, *40*, 1660.
- (18) Minceva-Sukarova, B.; Sherman, W. F.; Wilkinson, G. R. *J. Phys. C* **1984**, *17*, 5833.
- (19) Wong, P. T. T.; Whalley, E. *J. Chem. Phys.* **1976**, *64*, 2359.
- (20) Salzmann, C.; Kohl, I.; Loerting, T.; Mayer, E.; Hallbrucker, A. *J. Phys. Chem. B* **2002**, *106*, 1.
- (21) Abe, K.; Ishii, K.; Nakajima, M.; Fukuda, H.; Shigenari, T. *Ferroelectrics* **2000**, *239*, 1.
- (22) Minceva-Sukarova, B.; Slark, G. E.; Sherman, W. F. *J. Mol. Struct.* **1986**, *143*, 87.
- (23) Minceva-Sukarova, B.; Slark, G. E.; Sherman, W. F.; Wilkinson, G. R. *J. Phys.* **1987**, *Colloque C1*, 37.
- (24) Pruzan, P.; Chervin, J. C.; Canny, B. *J. Chem. Phys.* **1992**, *97*, 718.
- (25) Goncharov, A. F.; Struhkin, V. V.; Ho-kwang, M.; Hemley, R. J. *Phys. Rev. Lett.* **1999**, *83*, 1998.

- (26) Hirsch, K. R.; Holzapfel, W. B. *J. Chem. Phys.* **1986**, *84*, 2771.
- (27) Bertie, J. E.; Francis, B. F. *J. Chem. Phys.* **1980**, *72*, 2213.
- (28) Kohl, I.; Mayer, E.; Hallbrucker, A. *Phys. Chem. Chem. Phys.* **2001**, *3*, 602.
- (29) Mishima, O.; Calvert, L. D.; Whalley, E. *Nature* **1984**, *310*, 393.
- (30) Mishima, O.; Calvert, L. D.; Whalley, E. *Nature* **1985**, *314*, 76.
- (31) Koza, M. M.; Schober, H.; Hansen, T.; Tölle, A.; Fujara, F. *Phys. Rev. Lett.* **2000**, *84*, 4112.
- (32) Whalley, E.; Bertie, J. E. *J. Chem. Phys.* **1967**, *46*, 1264.
- (33) Yoshimura, Y.; Kanno, H. *Chem. Phys. Lett.* **2001**, *349*, 51.
- (34) Yoshimura, Y. Private communication.
- (35) Whalley, E. *Can. J. Chem.* **1977**, *55*, 3429.
- (36) Bertie, J. E.; Calvert, L. D.; Whalley, E. *Can. J. Chem.* **1963**, *38*, 840.
- (37) Kohl, I.; Mayer, E.; Hallbrucker, A. *J. Phys. Chem. B* **2000**, *104*, 12102.
- (38) Devlin, J. P.; Woolridge, P. J.; Ritzhaupt, G. *J. Chem. Phys.* **1986**, *84*, 6095.
- (39) Kuhs, W. F.; Lehmann, M. S. The Structure of Ice-Ih. In *Science Reviews 2*; Franks, F., Ed.; Cambridge University Press: Cambridge, 1986; Vol. 2; p 1.
- (40) Fleissner, G.; Hage, W.; Hallbrucker, A.; Mayer, E. *Appl. Spectrosc.* **1996**, *50*, 1235.
- (41) Vandeginste, B. G. M.; L., D. G. *Anal. Chem.* **1975**, *47*, 2124.
- (42) Gans, P.; Gill, J. B. *Anal. Chem.* **1980**, *52*, 351.
- (43) *Infrared and Raman Spectroscopy*; Schrader, B., Ed.; VCH Verlagsgesellschaft mbH: Weinheim, Federal Republic of Germany, 1995.